Journal of Ginseng Research 48 (2024) 464–473

Contents lists available at ScienceDirect

Journal of Ginseng Research

journal homepage: www.sciencedirect.com/journal/journal-of-ginseng-research

Research Article

The necessity of eliminating the interference of panaxatriol saponins to maximize the preventive effect of panaxadiol saponins against Parkinson's disease in rats

Yanwei Wang [a], Yufen Zhang [c], Yueyue Li [c], Zhizhen Zhang [b,*], Xiao-Yuan Lian [a,**]

[a] College of Pharmaceutical Sciences, Zhejiang University, Hangzhou, China
[b] Ocean College, Zhoushan Campus, Zhejiang University, Zhoushan, China
[c] Anhui University of Chinese Medicine, Hefei, China

ARTICLE INFO

Keywords:
Panaxadiol saponin fraction
Panaxatriol saponin fraction
Parkinson's disease

ABSTRACT

Background: The effects of individual panaxadiol saponin and panaxatriol saponin on rodent models of Parkinson's disease (PD) have been recognized. However, it is not clear whether purified total ginsenosides as an entirety has effect against PD in rat model. This study compared the protective effects of a purified panaxadiol saponin fraction (PDSF), a purified panaxatriol saponin fraction (PTSF), and their mixtures against the rotenone (ROT)-induced PD in rats.

Methods: Potential effects of PDSF, PTSF, and their mixtures against motor dysfunction and impairments of nigrostriatal dopaminergic neurons (DN), blood-brain barrier (BBB), cerebrovascular endothelial cells (CEC), and glial cells were measured in the models of ROT-induced PD rats and cell damage. Pro-inflammatory NF-kB p65 (p65) activation was localized in DN and other cells in the striatum.

Results: PDSF and PTSF had a dose-dependent effect against motor dysfunction with a larger effective dose range for PDSF. PDSF protected CEC, glial cells, and DN in models of PD rats and cell damage, while PTSF had no such protections. Chronic ROT exposure potently activated p65 in CEC with enhanced pro-inflammatory and decreased anti-inflammatory factors and impaired BBB in the striatum, PDSF almost completely blocked the ROT-induced p65 activation and maintained both anti- and pro-inflammatory factors at normal levels and BBB integrity, but PTSF aggravated the p65 activation with impaired BBB. Furthermore, PTSF nullified all the effects of PDSF when they were co-administrated.

Conclusion: PDSF had significant protective effect against the ROT-induced PD in rats by protecting CEC, glial cells, and DN, likely through inhibiting NF-κB p65 in CEC from triggering neuroinflammation, and also directly protecting glial cells and neurons against ROT-induced toxicity. PDSF has great potential for preventing and treating PD.

1. Introduction

Parkinson's disease (PD) is the second most common neurodegenerative disease globally, causing severe movement impairments and non-motor symptoms in patients [1]. Current treatment for PD is symptomatic typically with levodopa preparations prescribed with or without other medications [2]. To date, no therapy can slow down or arrest the progression of PD [1]. Evidences from epidemiological studies and animal models indicate that pesticide exposure substantially increases the PD risk by the inhibition of mitochondrial complex I (MCI) or causing oxidative stress [3,4]. Intragastric or subcutaneous administration of a pesticide rotenone (ROT), a well-known MCI inhibitor, can almost completely reproduce the typical pathological and clinical features of PD in rodents and is widely used to induce rodent models of PD for investigating the underlying mechanisms leading to PD and evaluating the new potential therapies for PD [3,5,6]. The pathogenesis of PD is complex and the MCI-mediated mitochondrial dysfunction, oxidative stress, and neuroinflammation likely due to activated microglia and impaired astrocytes all contribute to the degeneration of the nigrostriatal dopaminergic pathway [7]. Elevated extracellular glutamate

* Corresponding author. Ocean College, Zhoushan Campus, Zhejiang University, Zhoushan 316021, China.
** Corresponding author. College of Pharmaceutical Sciences, Zhejiang University, Hangzhou 310058, China.
E-mail addresses: zzhang88@zju.edu.cn (Z. Zhang), xylian@zju.edu.cn (X.-Y. Lian).

https://doi.org/10.1016/j.jgr.2024.05.002
Received 17 November 2023; Received in revised form 10 May 2024; Accepted 10 May 2024
Available online 14 May 2024

levels due to both an increased release and a decreased uptake by astrocytes in the substantia nigra and the striatum also accelerates the nigrostriatal dopaminergic degeneration and promotes the motor and no-motor symptoms as well as levodopa-induced dyskinesia [8–10]. Furthermore, cerebrovascular damage also promotes the progression of PD and causes vascular parkinsonism [11,12]. Therefore, it is important to protect neurons, glia, and cerebral vessels for the development of new drugs that can prevent PD and slow down or arrest the progression of PD.

Ginsenosides are the main active ingredients of ginseng (the root of *Panax* species) and mainly include panaxadiol saponins with ginsenosides Rb1, Rb2, Rb3, Rc, and Rd (GRb1, GRb2, GRb3, GRc, and GRd) as the major individuals and panaxatriol saponins with GRg1 and GRe as the major individuals [13,14]. These major ginsenosides have been demonstrated to have wide pharmacological activities on the central nervous system [15,16]. For examples, individual panaxatriol saponin Rg1 has nerve excitatory effects through activating excitatory receptors including glutamate receptor [17] and acetylcholine receptor [18]. While individual panaxadiol saponin GRb1 has the inhibitory effects likely by activating inhibitory γ-aminobutyric acid (GABA) receptors [19] and also inhibiting excitatory N-methyl-D-aspartic acid receptor (NMDA) receptors [20]. However, both GRb1 and GRg1 have been reported to be neuroprotective in animal models of PD and other neurodegenerative diseases [21], cerebral ischemic injury [22], and ischemic stroke [23]. It is also noticed that most of the previous reports on the pharmacological effects of ginsenosides on the central nervous system were focused on the individual ginsenosides. Here, it is reasonable to believe that the efficacy of an individual ginsenoside is not good as that of a combination of similar monomers. Indeed, our previous investigations demonstrated that a highly purified panaxadiol saponin fraction (PDSF) had significant protective activity against excitotoxicity and excitatory disorders, while a highly purified panaxatriol saponin fraction (PTSF) was inactive and even weaken the effects of PDSF [24,25]. Given that excitotoxicity plays an important role in the degeneration of the nigrostriatal dopaminergic pathway and the expression of motor symptoms of PD and levodopa-induced dyskinesia [8–10], this difference between the two types of ginsenosides reminds us to consider whether PDSF are more effective than PTSF for the prevention and treatment of PD.

Thus, this study compared the potential effects of PDSF, PTSF, and their mixture (PDSF + PTSF) against the onset and progression of ROT-induced PD in rats in order to identify the most effective faction for the development of new drug for the prevention and treatment of PD.

2. Materials and methods

2.1. Reagents and materials

Panaxadiol saponin fraction (PDSF) and panaxatriol saponin fraction (PTSF) were prepared in authors' laboratory as previously described method [26]. PDSF composed of five panaxadiol saponins (GRb1 35.37 %, GRb2 6.59 %, GRb3 13.98 %, GRc 13.19 %, and GRd 24.09 %) with total saponins of 93.23 %. PTSF composed of two panaxatriol saponins (GRe 89.60 % and GRg1 1.42 %) with total saponins of 91.02 %. Nerve growth factor (NGF), rotenone (ROT, ≥95 %), sulforhodamine B (SRB), fluorescein isothiocyanate (FITC) and trichloroacetic acid (TCA) were obtained from Sigma-Aldrich (USA). Monoclonal antibodies were purchased from the companies below: glial fibrillary acidic protein (GFAP), tyrosine hydroxylase (TH), and HRP-conjugated secondary antibodies (Proteintech, China); NF-κB p65, p–NF–κB p65 and ionized calcium-binding adapter molecule 1 (IBA1) antibodies (Invitrogen, USA); α-synuclein (α-Syn), p-α-Syn, complement component 3 (C3D) and platelet endothelial cell adhesion molecule-1 (CD31) antibodies (Abcam, USA). Bovine serum albumin (BSA) and skim milk were purchased from Sangon Biotech (China). Lysis buffer was purchased from Beyotime Biotechnology (China). Enhanced chemiluminescence (ECL) reagent and bicinchoninic acid (BCA) protein assay kit were purchased from Bio-Rad (USA). Phosphate buffered saline (PBS), roswell park memorial institute-1640 (RPMI-1640), dulbecco's modified eagle medium (DMEM), DMEM/F12, and fetal bovine serum (FBS) were purchased from Thermo Fisher Scientific (USA). Penicillin and streptomycin were ordered from YEASEN (China). TNF-α, IL-1β, IL-4, IL-6, and IL-10 ELISA kits were obtained from MlBio (China).

2.2. Rotenone-induced Parkinson's disease rat model and drug treatment

Male Sprague Dawley (SD) rats (n = 90; body weights at time of testing: 300 ± 20 g) were obtained from the Laboratory animal center of Zhejiang University (Hangzhou, Zhejiang province, China). All animals were housed in a standard environment under controlled conditions (22 ± 2 °C, a 12 h light/dark cycle) with food and water *ad libitum*. All procedures involving animals and their care were approved by the Zhejiang University Animal Experimentation Committee and followed the National Institutes of Health Guide for the Care and Use of Laboratory Animals. All surgeries were performed under urethane anesthesia and all efforts were made to minimize suffering.

Referring to previous literature [6], a ROT-induced PD pathological model was established in SD rats. Briefly, rats received a subcutaneous injection of rotenone (0.5 mg/mL rotenone dissolved in sunflower oil) twice one day (8:30 a.m. and 8:30 p.m.) at the back of the neck using the following dosages: 0.5 mg/kg (body weight, days 1–5), 0.625 mg/kg (days 6–10), and 0.75 mg/kg (days 11–15). The naive group received an injection of sunflower oil (1 mL/kg body weight) that did not include rotenone.

The SD rats were divided into naive group (n = 10), three PDSF groups (20, 40, and 60 mg/kg, dissolved in reverses osmosis (RO) water, each n = 10), three PTSF groups (20, 40, and 60 mg/kg, dissolved in RO water, each n = 10), and PDSF + PTSF group (PDSF 40 mg/kg + PTSF 40 mg/kg, n = 10). The drugs were administrated by gavage 30 min before the injection of rotenone. Naive animals received the same volume of RO water.

2.3. Behavior tests

Rats were habituated to the dimly lit and sound-proofed testing room for 60 min before the start of each assay.

Rota-Rod Test. An accelerating rotarod apparatus (Hugo Basile, Gemonio, Italy) was used for the Rota-Rod test as previously described [27]. The animals were trained 3 days before the test. Data are presented as the mean duration (three trials) on the rotarod.

Cylinder Test. Slight adjustments based on previously described [27] were made for the cylinder test. Briefly, spontaneous movement was measured by placing rats in an opaque cylindrical barrel with a height of about 30 cm and a diameter of about 20 cm. Spontaneous activity was recorded for 5 min. The numbers of forepaw touches, rears and grooming were measured. Recorded the number of times the rat's forelegs are lifted according to the standard of lifting the rat's forelegs over the shoulders and touching the barrel walls on both sides. Data are presented as a percentage relative to Naive animals: Rears % (per 1 min) = the numbers of forepaw touches within 1 min in the treatment group/the numbers of forepaw touches within 1 min in the Naive group × 100 %.

Forepaw adjusting steps (FAS) Test. FAS Test was referred to previous reported method [28]. The experiment was conducted with two experimenters who were blinded to treatment condition. The experimenter fixed and lifted the rat's hind limb skeleton with one hand and fixed its right forelimb with the other hand, so that the left forelimb foot was placed on the table. The rat's body was at an angle of about 45° from the table. Then, the rats were artificially adjusted to move at a constant speed of 90 cm/10 s along the edge of the table and each time at an interval of 10 s. Rats were dragged for 6 trials per forepaw: 3 backhand (lateral steps away from the torso) and 3 forehand (lateral steps toward

the torso) trials, alternating the starting forepaw between animals. Data are presented as a percentage relative to Naive animals: Steps in 90 cm % (per 10 s) = the numbers of forepaw steps within 10 s in the treatment group/the numbers of forepaw steps within 10 s in the Naive group × 100 %.

2.4. Immunohistochemistry and immunofluorescence

After the last behavioral test, animals were deeply anesthetized and perfused through the heart with 4 % buffered paraformaldehyde (PFA) of 100 mL. Brains were removed and fixed with 4 % PFA overnight. Coronal sections (50 μm) were cut with a vibratome (VT1000S, Leica, Germany) and the sections of the striatum and substantia nigra compacta (SNc) were collected. Free-floating brain sections were blocked with 4 % BSA/PBS plus 0.2 % Triton- 100 and incubated with primary antibody overnight at 4 °C, including TH, GFAP, IBA1, NF-κB p65 and CD31 antibodies, followed by the corresponding biotinylated secondary antibody or the one conjugated with fluorescent dyes. Images were obtained using microscope (Eclipse 50i, Nikon) or confocal microscope (Olympus BX61W1-FV1000).

For semi-quantitative analysis of the lesion volume in which TH immunoreactivity was lost in the striatum and the number of TH-positive neurons in the SNc, every 10th section through the entire striatum or SNc was stained for TH immunoreactivity. The lesion volume was estimated using Image J software. At least five sections evenly spaced through the lesion volume were measured for each animal. The actual distance between sections used for measurements depended on the extent of the lesion. The lesion volume was estimated using the following formula: volume = (a1 + a2, …+ a_n)/n × d, where d = distance (in millimeters) between sections, and a1, a2, a3, …= area (in square millimeters) of the lesion for individual sections [24]. To assess the numbers of TH-positive neurons in the SNc, images captured by the microscope were saved as tiff files, then magnified 1000× on a computer screen to facilitate cell count.

2.5. Immunoblot analysis

The striatum of three rats in each experimental group were homogenized and prepared in lysis buffer [(10 mM Tris-HCl, pH 7.3), 150 mM NaCl, 5 mM ethylene diamine tetra acetic acid, 1 % Nonidet P-40 (vol/vol), 1 % Triton-100, and 0.5 % sodium deoxycholic acid (wt/vol)]. The striatal tissue lysates (40 μg protein) were electrophoresed on SDS-PAGE gels and transferred to PVDF membranes. Membranes were blocked with 5 % skim milk (wt/vol) in TBS-T and incubated with the primary antibodies. After HRP-conjugated secondary antibody incubation, the immunoblot signal was detected using super ECL detection reagent and the targeted protein levels were quantified using Image J software.

2.6. Detection of vascular permeability using FITC-labeled bovine serum albumin

Bovine serum albumin (BSA) was labeled with FITC. Briefly, BSA was dissolved in a buffer ($V_{0.15\ mol/L\ NaCl}$: $V_{0.15\ mol/L\ NaHCO3–Na2CO3}$ = 9: 1) and the final protein concentration was adjusted to 10 mg/mL. Then, FITC powder was added and dissolved into the above solution until to the ratio of protein (mg): FITC (mg) = 50: 1 and incubated in the dark at 4 °C on a shaking table overnight. Then, the solution was transferred to a Millipore ultrafiltration tube, which can intercept molecules with molecular weight greater than 3 KD, and centrifuged at 5000 *g* for 2 h. After discarding the filtrate, the Millipore ultrafiltration tube was washed with the buffer for 3 times followed by using the buffer to dissolve FITC-labeled BSA and obtain the FITC-labeled BSA solution (10 mg/mL). After the last behavioral test, the rats were rapidly perfused with 4 % PFA in 0.1 M PBS (pH 7.2) after brief perfusion of PBS (pH 7.2) containing 5 U/ml heparin, and then perfused with 10 mL of the FITC-labeled BSA solution. The brains were dissected, post fixed in 4 % PFA in 0.1 M PBS (pH 7.2) at 4 °C for one week. Coronal sections (50 μm) were cut with a vibratome (VT1000S, Leica, Germany) and the sections of the striatum and SNc were collected and the distribution status of the FITC-labeled BSA were observed using a Nikon microscope.

2.7. Cell culture

According to reported method [29], PC12 cells were differentiated to dopaminergic neurons in the differentiation medium of RPMI-1640 supplemented with 100 ng/mL NGF, 10 % FBS, 50 U/mL penicillin, and 50 μg/mL streptomycin for 14 day. The culture medium was changed every 48 h bEnd.3 and HCVEC cells were cultured in high glucose DMEM medium supplemented with 10 % FBS, 50 U/mL penicillin, and 50 μg/mL streptomycin. All cells were maintained in a 5 % humidified CO_2 incubator at 37 °C.

2.8. Detection of inflammatory factor levels in the striatum and plasma using ELISA kits

The striatum was homogenized and prepared in lysis buffer [10 mM Tris-HCl, pH 7.3, 150 mM NaCl, 5 mM ethylene diamine tetra acetic acid, 1 % Nonidet P-40 (vol/vol), 1 % Triton × 100, and 0.5 % sodium deoxycholic acid (wt/vol)]. Protein levels were quantified using a BCA protein assay kit. According to the instructions of the reagent manufacturer, the levels of TNF-α, IL-1β, IL-6, IL-4 and IL-10 in tissue lysate were detected by ELISA kits.

2.9. Primary astrocyte culture

Primary astrocyte (PA) cultures were performed from rat pups at postnatal day 1 (P1) according to the previously reported method [30]. Representative sample cultures were stained for GFAP to verify that they were astrocyte cells.

2.10. Cell viability assay

Cell viability was measured using the SRB method according to previous report [31]. Briefly, cells were incubated overnight in 96-well plates with a cell density of 3000 per well until the cells were completely adhered. Cells were pretreated with different concentrations of test reagents for 3 h, followed by the addition of rotenone at IC_{50}, and then the cells were cultured for 48 h. Cell viability was measured by SRB.

2.11. Statistics

Data were analyzed by Two-way analysis of variance (ANOVA), followed by Tukey's multiple comparison test for multiple group comparisons, using GraphPad Prism software (GraphPad Software Inc., La Jolla, CA, USA). Data are expressed as the mean ± SEM and $p < 0.05$ is considered statistically significant.

3. Results

3.1. PDSF had a wider therapeutic dose range than PTSF in rotenone-induced PD rat model

Firstly, we observed the dose-effect relationship between PDSF and PTSF in the prevention and progression of PD in ROT-induced rat model. As shown in Fig. 1A in the Cylinder Test, with the prolongation of exposure to rotenone, the forelimb lifting ability of the model group (ROT) animals significantly decreased, almost reaching its lowest value by 13 days, when compared to the normal group (Naive) animals. Moreover, when tested 48 h after the last dose of rotenone, there was no significant increase in forelimb lifting ability compared to the previous measurement, indicated that this decrease in motor function was not a temporary change in motor behavior, but a manifestation of impaired

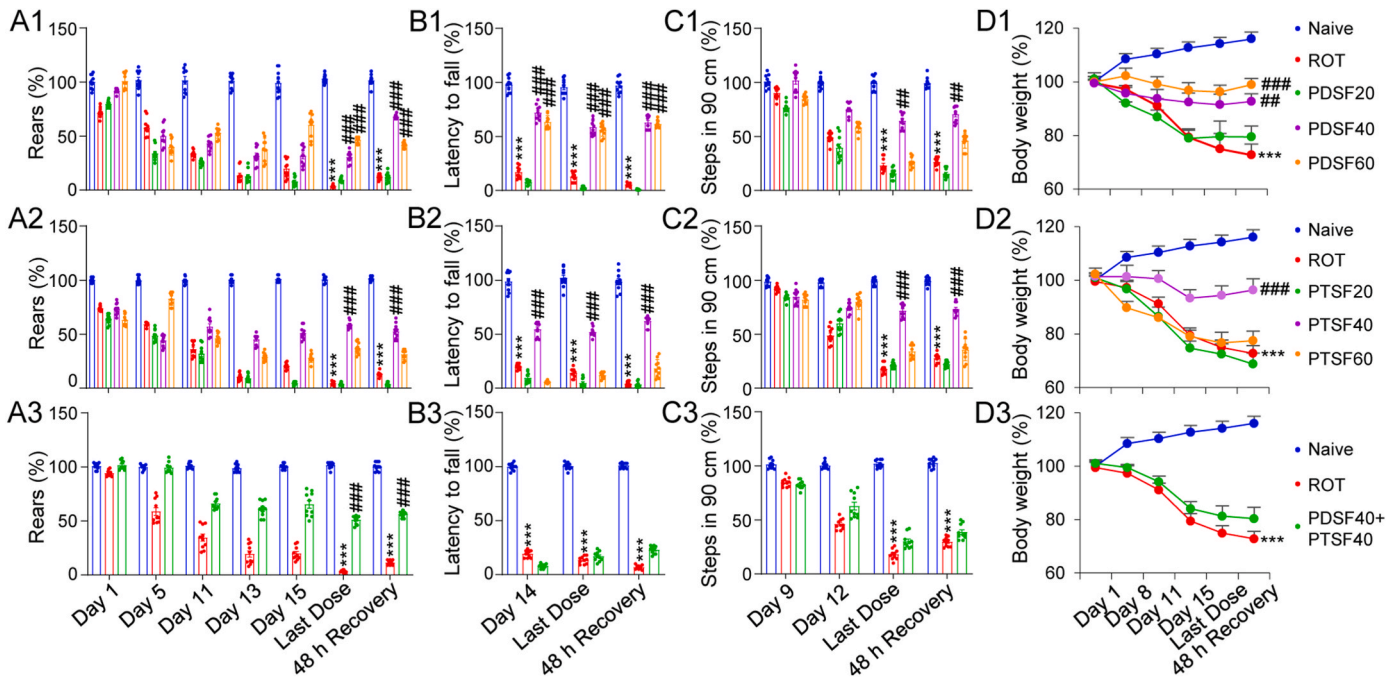

Fig. 1. PDSF had a wider therapeutic dose range than PTSF in RO-induced PD rat model. Results of animals on the rears (A), rotarod (B), FAS (C), and body weight (D). Data are presented as the mean ± SEM (n = 10), $^{*}P < 0.05$, $^{**}P < 0.01$, $^{***}P < 0.001$ vs Naive; $^{\#}P < 0.05$, $^{\#\#}P < 0.01$, $^{\#\#\#}P < 0.001$ vs ROT.

motor function. Administration of PDSF 1 h before each injection of rotenone can counteract the ROT-induced forelimb lifting dysfunction in a dose-dependent manner. In detail, PDSF 20 (a dose of 20 mg/kg/day) showed no significant improvement in ROT-induced impairment of forelimb lifting ability in rats; while PDSF 40 (40 mg/kg/day) and PDSF 60 (60 mg/kg/day) significantly antagonized ROT-induced decrease in forelimb lifting ability and the efficacy of PDSF 40 was better than that of PDSF 60. However, unlike PDSF, PTSF only improved the ability to lift the forelimbs of rats at a dose of 40 mg/kg (Fig. 1A2) and its efficacy was lower than that of PDSF 40. Due to the completion of each of the three set motor behavior tests taking more than 3 h, there is significant physical exertion on the animals during this process. Thus, we chose the time points that can reflect the efficacy of PDSF and PTSF in the Cylinder Test for Rota-Rod Test and FAS Test. Similar results (Fig. 1B2, C2) were also obtained from the Rota-Rod and FAS Tests. In the Rota-Rod Test, 40 mg/kg or 60 mg/kg PDSF significantly improved motor coordination against the neurotoxicity of rotenone (Fig. 1B1), while in the FAS Test PDSF was only effective at 40 mg/kg (Fig. 1C1). Clearly, the data indicated that 40 (mg/kg/day) was the optimum dose of PDSF in these set of tests. In addition, body weight is an important indicator for measuring the overall health status of animals. Therefore, we also tested the dynamic changes in body weight of all the animals (Fig. 1D). Consistent with the motor function indicators, the body weight of the ROT model animals gradually decreased until to 80 % at 15 days, while the weight of the naive animals increased by 10 %. Both PDSF 40 and PDSF 60 significantly counteracted the weight loss caused by rotenone and maintained animal weight at initial levels (Fig. 1D1), while PTSF had the similar effect at only at 40 mg/kg/day (Fig. 1D2). The above results indicated that both PDSF and PTSF counteracted ROT-induced PD symptoms and weight loss in a dose-dependent manner and 40 mg/kg/day was the optimal dose for both PDSF and PTSF, but the effective dose range of PDSF is wider than that of PTSF.

In order to reveal the possible interactions between PDSF and PTSF, including superimposed, synergistic or antagonistic effects, we measured the effects of a mixture of PDSF and PTSF at their optimal dose (40 mg/kg/day) on the above pharmacodynamic indicators. As shown in Fig. 1A3, B3, C3, and D3, the mixture did not have any protective effects on motor function indicators and weight loss. The results indicated that the protective effects of PDSF and PTSF were completely cancelled out when they are combined at their respective optimal dose or the equal dose.

3.2. *PDSF effectively counteracted the rotenone-induced dopaminergic nerve damage, while PTSF had no such effect and even weakened the effect of PDSF*

In order to further investigate the pharmacodynamic differences between PDSF and PTSF in improving the occurrence and progression of PD, we observed the state of the dopaminergic neural pathway and the aggregation of α-Syn in the substantia nigra and striatum of animals in each group by immunohistochemistry and western blotting analysis, whose degeneration were the neuropathological basis of PD. The results indicated that the ROT-induced PD rats showed a significant loss of TH staining in both dorsal lateral part of the striatum and below the SNc (Fig. 2A and B), but there was no significant decrease in the dopaminergic neuron soma in the substantia nigra compacta, indicated the damages of dopaminergic nerve endings and the ability to synthesize dopamine in the striatum, as well as the damage of dopaminergic nerve dendrites in the substantia nigra. The western blotting analysis also showed that the TH levels in the striatum of PD rats were significantly lower than those in the striatum of naive animals (Fig. 2C). In addition, the western blotting analysis also showed that the p-α-Syn levels in the striatum of ROT-induced PD rats were significantly higher than those in the striatum of naive animals, which suggested the aggregation of α-Syn in the striatum of PD rats (Fig. 2D). PDSF (40 mg/kg/day) significantly protected the dopaminergic neural pathway and reduced the aggregation of α-Syn in the substantia striatum and SNc at effective doses of motor behavior. It is worthwhile to notice that PTSF (40 mg/kg/day) did not have significant neuroprotective effects at the effective dose of motor behavior, consistent with a loss of TH staining in multiple regions of the striatum (Fig. 2A and B) and the aggregation of α-Syn in the striatum (Fig. 2D). In line with the results of motor behavioral tests, the mixture PDSF + PTSF did not show significant neuroprotective effects, indicating that the simultaneous use of equal dose of PTSF and PDSF counteract the protective effect of PDSF against ROT-induced dopamine nerve damage. The above results indicated that PDSF significantly

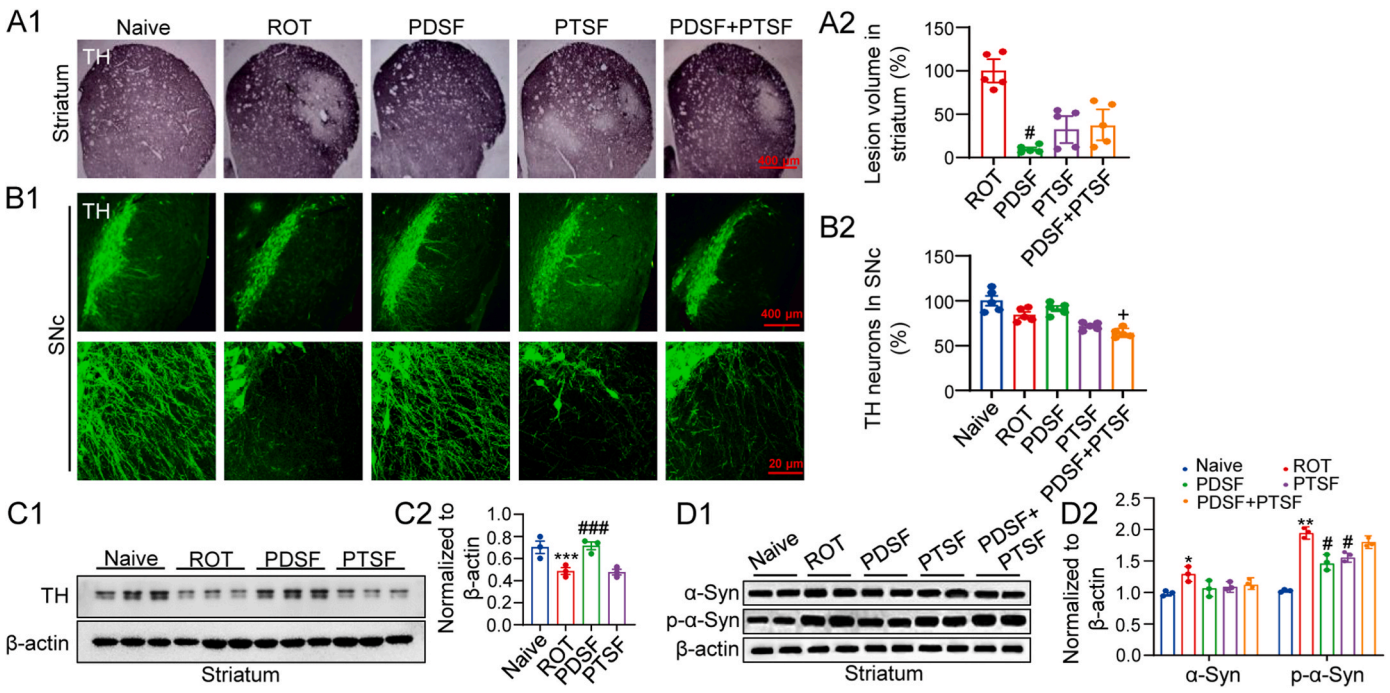

Fig. 2. PDSF effectively counteracted the ROT-induced dopaminergic nerve damage, while PTSF had no such effect and even weakened the effect of PDSF. A1: Representative TH immunohistochemistry in the striatum. A2: Quantification of striatum dopamine nerve fibers lesion volume. B1: Representative TH immunostaining (green) in the SNc. B2: Quantification of dopamine neurons in SNc. Data are presented as the mean ± SEM (n = 5), $^{\#}P < 0.05$ vs ROT; $^{+}P < 0.05$ vs PDSF40. C1: Representative immunoblots of TH and β-actin in the striatum. C2: Quantification of TH levels in the striatum normalized to β-actin. D1: Representative immunoblots of α-Syn and *p*-α-Syn in the striatum. D2: Quantification of α-Syn and p-α-Syn levels in striatum normalized to β-actin. Data are presented as the mean ± SEM (n = 3), $^{*}P < 0.05$, $^{**}P < 0.01$, $^{***}P < 0.001$ vs Naïve; $^{\#}P < 0.05$, $^{\#\#}P < 0.01$, $^{\#\#\#}P < 0.001$ vs ROT.

protected the nigrostriatal dopaminergic pathway against the neurotoxicity of mitochondrial complex I inhibitor rotenone, while PTSF did not have this neuroprotective effect and even completely counteracted the protective effect of PDSF.

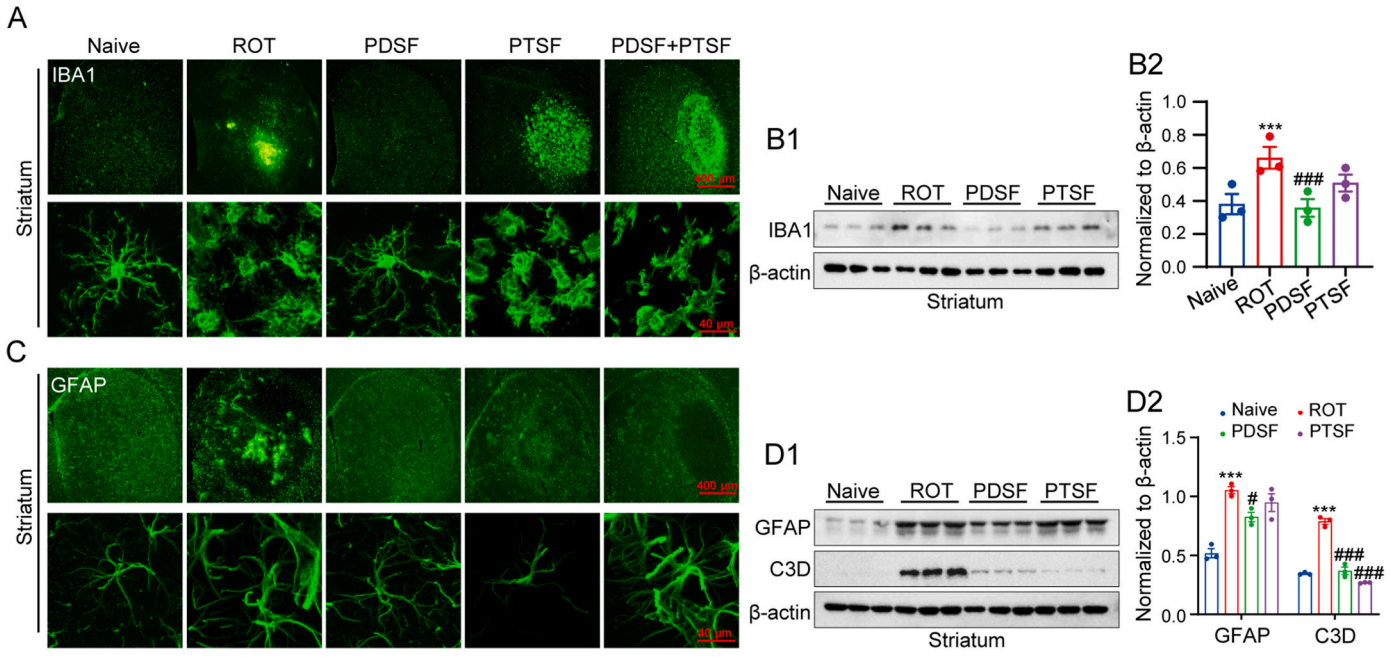

Fig. 3. PDSF effectively counteracted the ROT-induced glial cell injury, while PTSF partially protected astrocytes but impaired the protective effect of PDSF. A: Representative IBA1 immunostaining (green) in the striatum. B1: Representative immunoblot results of IBA1 and β-actin in the striatum. B2: Quantification of IBA1 levels in striatum normalized to β-actin. C: Representative GFAP immunostaining (green) in the striatum. D1: Representative immunoblot results of GFAP, C3D, and β-actin in the striatum. D2: Quantification of C3D levels in striatum normalized to β-actin. Data are presented as the mean ± SEM (n = 3). $^{**}P < 0.01$, $^{***}P < 0.001$ vs Naïve; $^{\#}P < 0.05$, $^{\#\#}P < 0.01$, $^{\#\#\#}P < 0.001$ vs ROT.

3.3. PDSF effectively counteracted rotenone-induced glial cell injury, while PTSF partially protected astrocytes but impaired the protective effect of PDSF

Based on the widespread involvement of glial cells in the occurrence and progression of PD [32,33], we observed the state of microglial cells and astrocytes in the striatum in each group using immunohistochemistry and western blotting analysis to further reveal possible differences in pharmacodynamic differences between PTSF and PDSF. As shown in Fig. 3A, in the dorsal lateral striatum of ROT-induced PD rats, IBA1 staining exhibited large numbers of activated microglia cells characterized by a swollen cell body with short and thick protrusions with significantly increased IBA1 (specific antibody for microglia) levels (Fig. 3B). PDSF (40 mg/kg/day) almost completely counteracted the ROT-induced excessive activation of microglia, while PTSF (40 mg/kg/day) did not show such effect, and the combination of PTSF and PDSF was neither effective, indicating that PTSF almost completely counteracted the effect of PDSF in inhibiting excessive activation of microglia.

As presented in Fig. 3C, the dorsolateral side of striatum of ROT-induced rats showed a circular lesion area with significant activation of astrocytes around the lesion area and loss of astrocytes in the center of the lesion area with an increase in GFAP levels and A1 type astrocytes that is neurotoxic and marked by C3D in whole striatum (Fig. 3D). Compared with the rotenone group, PDSF significantly protected astrocytes as indicated by alleviated activation of astrocytes and decreased C3D levels in the striatum (Fig. 3D), while PTSF only partially decreased astrocyte loss in the striatum with a decreased C3D levels in western blotting assay. However, the mixture PDSF + PTSF did not significantly improve the loss of astrocytes in the lesion area. In summary, the data demonstrated the robust protective effects of PDSF on both microglia and astrocytes, while PTSF only partially protected astrocytes, and particularly, PTSF largely weakened the effects of PDSF when it was combined with PDFS.

3.4. PDSF significantly inhibited the rotenone-induced NF-κB p65 signaling in cerebral vascular endothelial cells and PTSF seemly enhanced the NF-κB p65 signaling and counteracted the anti-inflammatory effect of PDSF

Neuroinflammation plays an important role in the occurrence and progression of PD and glial dysfunction, especially overactivated microglia, has been believed to trigger this neuroinflammation [34,35]. NF-κB-mediated inflammatory response was analyzed by measuring NF-κB p65 levels in the striatum of the relevant experimental animals by using immunohistochemistry and western blotting, attempting to reveal how PDSF inhibited the activation of microglia and how PTSF counteracted the effect of PDSF in ROT-induced PD rats. Strikingly, as shown in Fig. 4A, strong NF-κB p65 straining that presented vascular morphology showed in the striatum of rats in the groups of ROT, PTSF, and PDSF + PTSH, while there was no obvious NF-κB p65 staining in naive rats and PDSF-treated rats. These results were confirmed by western blotting analysis (Fig. 4B). When compared with naive control, the protein level of NF-κB p65 was significantly increased in the striatum in the ROT control group, with a stronger increase in the level of p–NF–κB p65. PDSF completely resisted the increases of the levels of NF-κB p65 and p–NF–κB p65, while PTSF showed mild effects against the p–NF–κB p65 increase, but PTSF when combined with PDSF completely canceled out these effects of PDSF. Next, the levels of NF-κB p65-driven inflammatory factors and anti-inflammatory factors in the striatum of rats were detected by using ELISA kits. Consistent with the changes in NF-κB p65 levels, the levels of pro-inflammatory factors including TNF-α, IL-1β, and IL-6 were dramatically increased, and the levels of anti-inflammatory factors IL-4 and IL-10 were significantly decreased in the ROT group compared to naive group (Fig. 4C); PDSF (40 mg/kg/day) completely prevented the alterations in the levels of pro-inflammatory factors and anti-inflammatory factors (Fig. 4C) in ROT-induced PD rats. However, PTSF (40 mg/kg/day) potently decreased the levels of the pro-inflammatory factors, but did not maintain the levels of IL-4 and IL-10 at the levels of naive rats (Fig. 4C),

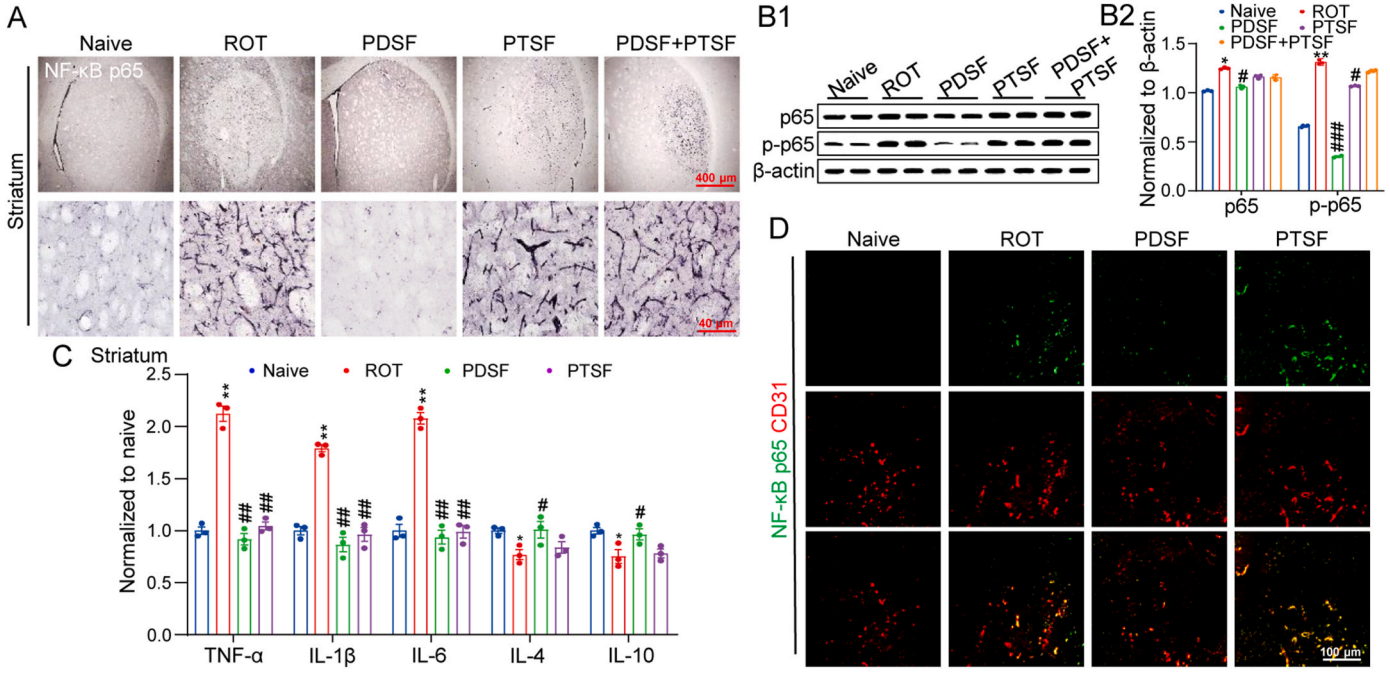

Fig. 4. PDSF significantly inhibited the ROT-induced NF-κB p65 signaling in cerebral vascular endothelial cells and PTSF seemly enhanced NF-κB p65 signaling and counteracted the anti-inflammatory effect of PDSF. A: Representative NF-κB p65 immunohistochemistry in the striatum. B1: Representative immunoblots of NF-κB p65 and p–NF–κB p65 in the striatum. B2: Quantification of NF-κB p65 and p–NF–κB p65 levels in striatum normalized to β-actin. Data are presented as the mean ± SEM. C: Detection of inflammatory factor levels in the striatum using ELISA. D: Representative double immunostaining NF-κB p65 (green) and CD31 (red) in the striatum (n = 3). $^{***}P < 0.001$ vs Naïve; $^{\#\#\#}P < 0.001$ vs ROT.

suggesting that decreased anti-inflammatory factors may contribute to the overactivated microglia in the PTSF-treated rats.

Finally, to confirm the activated NF-κB p65 occurred at vascular endothelial cells (Fig. 4A), colocalization of NF-κB p65 and CD31 (a vascular endothelial cell marker) were detected by immunofluorescence. The staining showed a complete colocalization of increased NF-κB p65 and CD31 in the striatum of rats in the ROT- and PTSF-treated groups (Fig. 4D). The results demonstrated that the NF-κB p65-mediated inflammatory response initially occurred in cerebral vascular endothelial cells of the ROT-induced PD rats.

Altogether, our data elucidated several points. Firstly, activated NF-kB pro-inflammatory response in cerebral vascular endothelial cells instead of predicted microglia may initiate neuroinflammation in the striatum and both elevated pro-inflammatory factors and decreased anti-inflammatory factors involve in neuroinflammation-mediated neuropathogenesis in ROT-induced PD rats. Secondly, PDSF inhibited the ROT-induced NF-κB p65 activation in cerebral vascular endothelial cells and maintained pro-inflammatory factors and decreased anti-inflammatory factors at the normal levels in the striatum, while PTSF promoted the ROT-induced NF-κB p65 activation in cerebral vascular endothelial cells, failed to maintain the levels of anti-inflammatory factors, and counteracted the effect of PDSF against the NF-κB p65-mediated pro-inflammatory response. These findings suggested an importance of protection of cerebral vascular endothelial cells for preventing ROT-induced PD.

3.5. PDSF protected the rotenone-induced impairment of the blood-brain barrier, while PTSF was unable to protect blood-brain barrier and weakened the inhibitory effect of PDSF

Cerebral vascular endothelial cells as an important component of the blood-brain barrier (BBB), in which the excessive inflammatory response often leaded to peripheral immune cell infiltration to the brain to exacerbate the development of neuroinflammation and diseases [36]. Therefore, we further measured the BBB damage in the striatum and substantia nigra by perfused rat hearts with FITC-labeled BSA. In general, vascular injury leads to FITC-BSA infiltration into perivascular tissues. As shown in Fig. 5, numerous FITC-BSA infiltrates were observed around the blood vessels in the striatum and substantia nigra of ROT-induced PD rats, indicating impairment of the BBB in the striatum of ROT-induced PD. PDSF (40 mg/kg/day) significantly reduced FITC-BSA infiltration into perivascular tissues and significantly protected the BBB, while PTSF (40 mg/kg/day) showed only a mild protective effect, and the mixture of PDSF + PTSF significantly attenuated the effect of PDSF. These data demonstrated that PDSF strongly protected BBB from the ROT-induced damage, therefore preventing broken BBB to trigger or promote PD onset or progression [36], while PTSF had no such protective effect and even impaired the effect of PDSF.

3.6. PDSF provided a direct protection of neurovascular unit cells against rotenone toxicity, while PTSF had no this protection and even weakened the efficacy of PDSF

As part of the neurovascular unit, blood-brain barrier (BBB) is anatomically comprised by brain microvascular endothelial cells, which along with pericytes, astrocytes, neuronal processes, perivascular microglia, and the basal lamina, form the neurovascular unit that is impaired in PD brain and in turn promotes the disease progression [37]. Thus, we further determined the potential differences among PDSF, PTSF, and their mixture in protective effects on vascular endothelial cells including bEnd.3 cells, HCVEC, primary astrocytes (PA), and PC12-differenated dopaminergic neurons (DN) against ROT-induced toxicity in cell culture. Firstly, in the normal culture condition, PDSF and PTSF did not affect the cell viability of the neurovascular unit cells at three different tested concentrations of 2.5, 5, and 10 μM, with an exception that PDSF at 10 μM promoted DN growth (Fig. 6A and B). In the culture medium with ROT at 0.4 μM for DN, 0.15 μM for bEnd.3, 1.2 μM for PA, and 0.1 μM for HCVEC, pre-treatment with PDSF for 3 h significantly protected all the tested cells at all the concentrations from the toxicity induced by rotenone exposure for 72 h, while PTSF had no such protections, and even impaired the protective efficacy of PDSF when it was combined with PDSF (Fig. 6C–F). These data indicated that PDSF was able to directly protect cerebrovascular endothelial cells, astrocytes, and dopaminergic neurons against the ROT-induced toxicity, while PTSF was not protective and even impaired the effect of PDSF. These results strongly supported the *in vivo* experimental results that PDSF significantly protected BBB, glial cells, and the nigrostriatal dopaminergic pathway, while PTSF had no such protective effects and weakened the effect of PDSF when PTSF and PDSF were co-administrated.

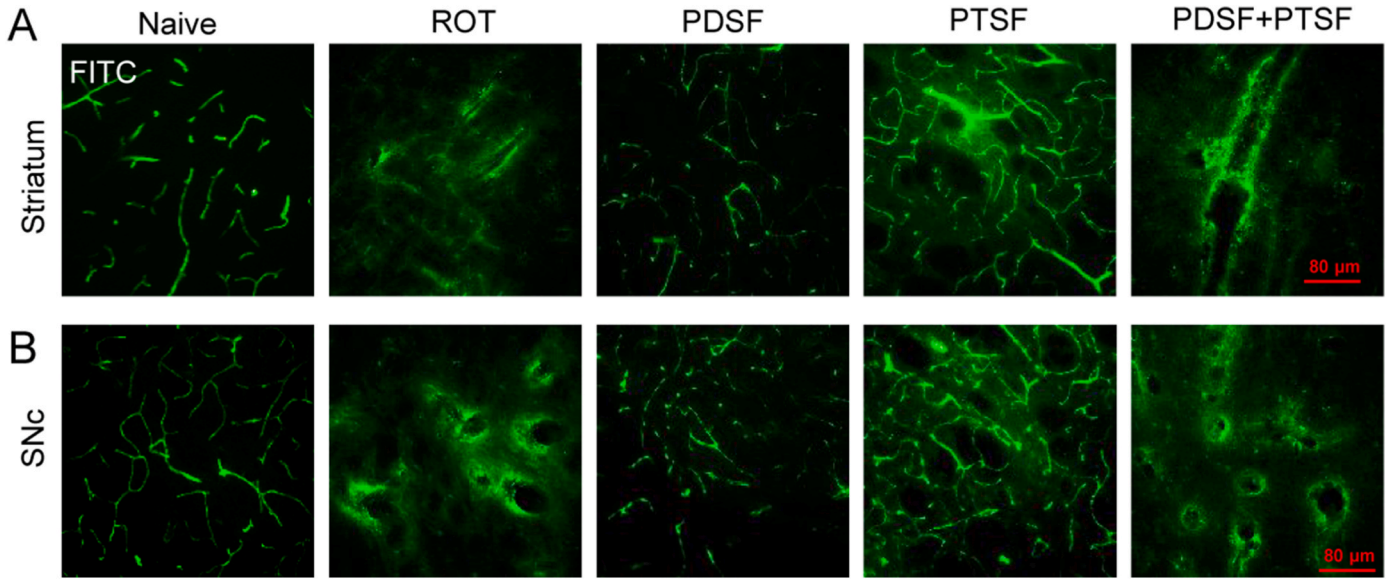

Fig. 5. PDSF protected the ROT-induced impairment of the blood-brain barrier (BBB) and inhibited invasion of peripheral immune cells, while PTSF was unable to protect BBB and weakened the inhibitory effect of PDSF. Representative FITC-BSA infiltrates image in the striatum and SNc of rats (n = 3).

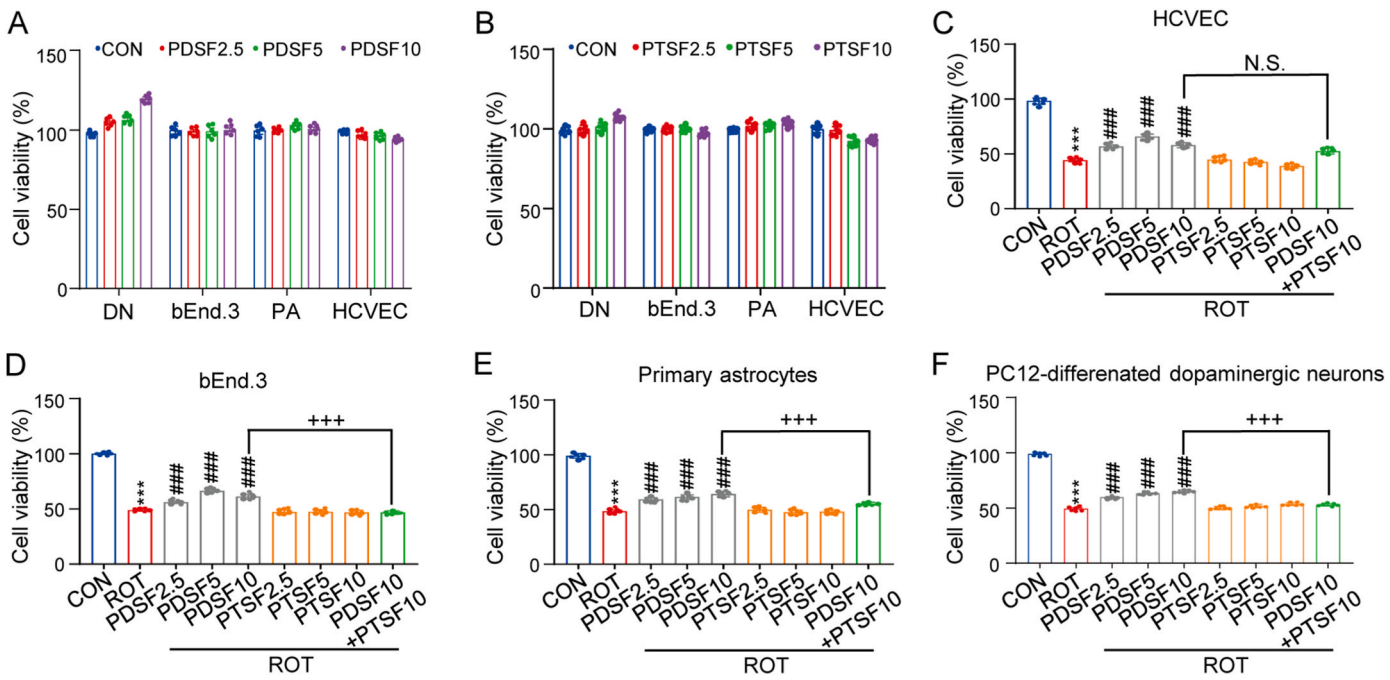

Fig. 6. PDSF provided a direct protection of neurovascular unit cells against ROT-induced toxicity, while PTSF had no such protection and even weakened the efficacy of PDSF. Cells were pretreated with PDSF, PTSF, and PDSF + PTSF for 3 h followed by rotenone (0.4 μM for DN; 0.15 μM for bEnd.3; 1.2 μM for PA; 0.1 μM for HCVEC). Cell viability was determined by the SRB assay (n = 6, biologically independent cells). Data are presented as the mean ± SEM. $^{**}P < 0.01$, $^{***}P < 0.001$ vs CON; $^{\#\#\#}P < 0.001$ vs ROT; $^{+++}P < 0.001$ vs PDSF.

4. Discussion

This study provided a new inspiration for the rational use of ginsenosides for the prevention and treatment of Parkinson's disease. The individual compound of the two types of ginsenosides (panaxatriol saponins and panaxadiol saponins) has been showed to have extensively pharmacological actions in central nervous system and was therefore widely considered to have the potential for the treatment of neurodegenerative diseases [15,16]. However, as the representatives of the central excitatory active and inhibitory active components in ginseng, panaxatriol saponins and panaxadiol saponins may show differences in their mechanisms of action and therapeutic effects against neurodegenerative diseases and the coexistence of the two types of ginsenosides may offset each other's respective effects [24,38,39]. Therefore, how to maximize the role of ginsenosides in preventing and treating neurological diseases is needed to be clarified. This study revealed the significant differences between the highly purified panaxadiol saponin fraction (PDSF) and panaxatriol saponin fraction (PTSF) in the pharmacological dose range and effects in the ROT-induced PD rat and cell models. Specifically, although both PDSF and PTSF effectively counteracted the motor dysfunction, PTSF was only effective at one dose of 40 mg/kg, while PDSF had a wider effective dose range. More importantly, PDSF significantly inhibited NF-κB pro-inflammatory response in cerebrovascular endothelial cells and thus prevented the activated NF-κB-mediated neuroinflammation and maintained the anti-inflammatory factor levels in the striatum, protected the BBB integrity from peripheral macrophage infiltration into the striatum where astrocytes and microglia were also protected, and protected the nigrostriatal dopaminergic pathway from chronic exposure to rotenone in rats. Moreover, PDSF was able to provide a direct protection to cerebrovascular endothelial cells, astrocytes, and dopaminergic neurons against ROT-induced cytotoxicity, indicating a potent protection of PDSF against the neurovascular units. By contrast, PTSF exacerbated the NF-κB pro-inflammatory response and was unable to maintain the levels of anti-inflammatory factors and to protect any cell type of the neurovascular units in the rats or the cell cultures. More importantly, PTSF potently impaired and even completely counteracted all the protective effects of PDSF when PTSF and PDSF were co-administrated. These findings indicated that a promising potential of PDSF for the prevention and treatment PD caused by environmental toxins and suggest that the mixture of panaxadiol saponins and panaxatriol saponins, especially at 1:1 wt ratio, should be avoided in the development of ginsenosides as new therapies for the prevention and treatment of PD and other neurodegenerative diseases.

Our findings revealed that PDSF could prevent or block the occurrence and progression of PD induced or triggered by environmental toxins such as rotenone from multiple aspects. Firstly, it is well known that environmental toxins such as rotenone or gene mutation-induced MCI dysfunction and neuroinflammation played key roles in the occurrence and progression of PD [34,35,40–43]. Secondly, BBB impairment that caused peripheral immune cells infiltration into the brain and insufficient blood supply [44], astrocyte dysfunction such as neurotoxic A1 cell formation [45], decreased extracellular glutamate uptake [46], and microglia-mediated neuroinflammation [47] all contribute to the nigra-striatal dopaminergic pathway degeneration. All these contributive events occurred in the ROT-induced PD rats and were prevented by PDSF. Additionally, our data indicated that activated NF-κB p65 signaling in cerebrovascular endothelial cells may start neuroinflammation and then the activation of microglia and the infiltrated peripheral immune cells could aggravate neuroinflammation in brain of the ROT-induced PD rats. Notably, PDSF not only directly protected BBB, cerebrovascular endothelial cells, astrocytes, and dopaminergic neurons, but also blocked NF-κB p65 signaling-mediated vicious cycle.

Our findings indicated that PDSF could decrease the risk of cerebrovascular damage in the occurrence and progression of PD. PD patients often experienced cerebrovascular damage [48]. Cerebrovascular damage promoted the progression of PD [12,37] and even caused the occurrence of vascular parkinsonism [11]. Therefore, the protection of BBB and cerebrovascular endothelial cells of PDSF made it to reduce the risk of cerebrovascular damage in the occurrence and development of PD.

5. Conclusion

This study demonstrates that the highly purified panaxadiol saponin fraction (PDSF) potently protected both motor function and brain histology, including BBB, cerebrovascular endothelial cell, microglia cells, astrocytes, and dopaminergic neurons, against PD induced by chronic rotenone exposure in rats, while PTSF not only fails to protect the brain histology but also nullified the effects of PDSF. As possible mechanism of the actions, PDSF inhibited the NF-κB-mediated pro-inflammatory response in cerebrovascular endothelial cells and then prevented neuroinflammation induced by the infiltration of peripheral immune cells and microglia cells. Therefore, PDSF as an entirety has great potential for the development of new medicine for the prevention and treatment of Parkinson's disease.

Author contributions

Xiao-Yuan Lian conceived, designed, and supervised this study. Yufen Zhang and Yanwei Wang performed the experiments. Yanwei Wang and Yueyue Li conducted the analysis and interpretation of data, Zhizhen Zhang prepared PDSF and PTSF, Xiao-Yuan Lian, Zhizhen Zhang, and Yanwei Wang wrote and revised the manuscript. All authors reviewed and approved the final manuscript.

Declaration of competing interest

The authors declare no conflict of potential conflicts of interest.

Acknowledgments

This work was supported by the National Natural Science Foundation of China (No. 82074039) and the Zhejiang Provincial Natural Science Foundation (Key project, No. LZ20H280001). We appreciate the Core Facilities of Zhejiang University School of Medicine for providing facilities.

References

[1] Bloem BR, Okun MS, Klein C. Parkinson's disease. Lancet 2021;397:2284–303.
[2] Armstrong MJ, Okun MS. Diagnosis and treatment of Parkinson Disease: a review. JAMA 2020;323:548–60.
[3] Klingelhoefer L, Reichmann H. Pathogenesis of Parkinson disease–the gut-brain axis and environmental factors. Nat Rev Neurol 2015;11:625–36.
[4] Ascherio A, Schwarzschild MA. The epidemiology of Parkinson's disease: risk factors and prevention. Lancet Neurol 2016;15:1257–72.
[5] Radad K, Al-Shraim M, Al-Emam A, Wang F, Kranner B, Rausch WD, Moldzio R. Rotenone: from modelling to implication in Parkinson's disease. Folia Neuropathol 2019;57:317–26.
[6] Betarbet R, Sherer TB, MacKenzie G, Garcia-Osuna M, Panov AV, Greenamyre JT. Chronic systemic pesticide exposure reproduces features of Parkinson's disease. Nat Neurosci 2000;3:1301–6.
[7] Przedborski S. The two-century journey of Parkinson disease research. Nat Rev Neurosci 2017;18:251–9.
[8] Majláth Z, Toldi J, Fülöp F, Vécsei L. Excitotoxic mechanisms in non-motor dysfunctions and levodopa- induced dyskinesia in Parkinson's disease: the role of the interaction between the dopaminergic and the kynurenine system. Curr Med Chem 2016;23:874–83.
[9] Marino BLB, de Souza LR, Sousa KPA, Ferreira JV, Padilha EC, da Silva C, Taft CA, Hage-Melim LIS. Parkinson's disease: a review from pathophysiology to treatment. Mini Rev Med Chem 2020;20:754–67.
[10] Rascol O, Fabbri M, Poewe W. Amantadine in the treatment of Parkinson's disease and other movement disorders. Lancet Neurol 2021;20:1048–56.
[11] Narasimhan M, Schwartz R, Halliday G. Parkinsonism and cerebrovascular disease. J Neurol Sci 2022;433:120011.
[12] Jacob MA, Cai M, Bergkamp M, Darweesh SKL, Gelissen LMY, Marques J, Norris DG, Duering M, Esselink RAJ, Tuladhar AM, et al. Cerebral small vessel disease progression increases risk of incident parkinsonism. Ann Neurol 2023;93:1130–41.
[13] Lee DY, Cho JG, Lee MK, Lee JW, Lee YH, Yang DC, Baek NI. Discrimination of Panax ginseng roots cultivated in different areas in Korea using HPLC-ELSD and principal component analysis. J Ginseng Res 2011;35:31–8.
[14] Liu J, Liu Y, Zhao L, Zhang ZH, Tang ZH. Profiling of ginsenosides in the two medicinal Panax herbs based on ultra-performance liquid chromatography-electrospray ionization-mass spectrometry. SpringerPlus 2016;5:1770.
[15] Kim HJ, Kim P, Shin CYA. Comprehensive review of the therapeutic and pharmacological effects of ginseng and ginsenosides in central nervous system. J Ginseng Res 2013;37:8–29.
[16] Lu J, Wang X, Wu A, Cao Y, Dai X, Liang Y, Li X. Ginsenosides in central nervous system diseases: pharmacological actions, mechanisms, and therapeutics. Phytother Res 2022;36:1523–44.
[17] Zhu G, Wang Y, Li J, Wang J. Chronic treatment with ginsenoside Rg1 promotes memory and hippocampal long-term potentiation in middle-aged mice. Neuron 2015;292:81–9.
[18] Jin Y, Peng J, Wang X, Zhang D, Wang T. Ameliorative effect of ginsenoside Rg1 on lipopolysaccharide-induced cognitive impairment: role of cholinergic system. Neurochem Res 2017;42:1299–307.
[19] Chen H, Shen J, Li H, Zheng X, Kang D, Xu Y, Chen C, Guo H, Xie L, Wang G, et al. Ginsenoside Rb1 exerts neuroprotective effects through regulation of Lactobacillus helveticus abundance and GABA(A) receptor expression. J Ginseng Res 2020;44:86–95.
[20] Chen WZ, Liu S, Chen FF, Zhou CJ, Yu J, Zhuang CL, Shen X, Chen BC, Yu Z. Prevention of postoperative fatigue syndrome in rat model by ginsenoside Rb1 via down-regulation of inflammation along the NMDA receptor pathway in the hippocampus. Biol Pharm Bull 2015;38:239–47.
[21] González-Burgos E, Fernandez-Moriano C, Gómez-Serranillos MP. Potential neuroprotective activity of ginseng in Parkinson's disease: a review. J Neuroimmune Pharmacol 2015;10:14–29.
[22] Xie W, Wang X, Xiao T, Cao Y, Wu Y, Yang D, Zhang S. Protective effects and network analysis of ginsenoside Rb1 against cerebral ischemia injury: a pharmacological review. Front Pharmacol 2021;12:604811.
[23] Zhao A, Liu N, Yao M, Zhang Y, Yao Z, Feng Y, Liu J, Zhou GA. Review of neuroprotective effects and mechanisms of ginsenosides from *Panax ginseng* in treating ischemic stroke. Front Pharmacol 2022;13:946752.
[24] Lian XY, Zhang Z, Stringer JL. Protective effects of ginseng components in a rodent model of neurodegeneration. Ann Neurol 2005;57:642–8.
[25] Xu K, Zhang Y, Wang Y, Ling P, Xie X, Jiang C, Zhang Z, Lian XY. Ginseng Rb fraction protects glia, neurons and cognitive function in a rat model of neurodegeneration. PLoS One 2014;9:e101077.
[26] Lian, XY, Zhang, ZZ, Zhao, Y, Wu, YY, Zheng, WT, Wang, ZW. Active ginsenoside composition and its preparation method and application in the preparation of drugs for preventing and/or treating diseases or health products with health benefits. Chinse patent, CN116019819A 2023-04-28.
[27] Yun SP, Kam TI, Panicker N, Kim S, Oh Y, Park JS, Kwon SH, Park YJ, Karuppagounder SS, Park H, et al. Block of A1 astrocyte conversion by microglia is neuroprotective in models of Parkinson's disease. Nat Med 2018;24:931–8.
[28] Chotibut T, Meadows S, Kasanga EA, McInnis T, Cantu MA, Bishop C, Salvatore MF. Ceftriaxone reduces L-dopa-induced dyskinesia severity in 6-hydroxydopamine Parkinson's disease model. Mov Disord 2017;32:1547–56.
[29] Wiatrak B, Kubis-Kubiak A, Piwowar A, Barg E. PC12 cell Line: cell types, coating of culture vessels, differentiation and other culture conditions. Cells 2020;9:958.
[30] Bramanti V, Bronzi D, Tomassoni D, Li Volti G, Cannavò G, Raciti G, Napoli M, Vanella A, Campisi A, Ientile R, et al. Effect of choline-containing phospholipids on transglutaminase activity in primary astroglial cell cultures. Clin Exp Hypertens 2008;30:798–807.
[31] Vichai V, Kirtikara K. Sulforhodamine B colorimetric assay for cytotoxicity screening. Nat Protoc 2006;1:1112–6.
[32] Halliday GM, Stevens CH. Glia: initiators and progressors of pathology in Parkinson's disease. Mov Disord 2011;26:6–17.
[33] Tremblay ME, Cookson MR, Civiero L. Glial phagocytic clearance in Parkinson's disease. Mol Neurodegener 2019;14:16.
[34] Kwon HS, Koh SH. Neuroinflammation in neurodegenerative disorders: the roles of microglia and astrocytes. Transl Neurodegener 2020;9:42.
[35] Wang Q, Zheng J, Pettersson S, Reynolds R, Tan EK. The link between neuroinflammation and the neurovascular unit in synucleinopathies. Sci Adv 2023;9:eabq1141.
[36] Belarbi K, Cuvelier E, Bonte MA, Desplanque M, Gressier B, Devos D, Chartier-Harlin MC. Glycosphingolipids and neuroinflammation in Parkinson's disease. Mol Neurodegener 2020;15:59.
[37] Iadecola C. The neurovascular unit coming of age: a journey through neurovascular coupling in health and disease. Neuron 2017;96:17–42.
[38] Lian XY, Zhang ZZ, Stringer JL. Anticonvulsant activity of ginseng on seizures induced by chemical convulsants. Epilepsia 2005;46:15–22.
[39] Lian XY, Zhang Z, Stringer JL. Anticonvulsant and neuroprotective effects of ginsenosides in rats. Epilepsy Res 2006;70:244–56.
[40] Liu Y, Yang H. Environmental toxins and alpha-synuclein in Parkinson's disease. Mol Neurobiol 2005;31:273–82.
[41] Pang SY, Ho PW, Liu HF, Leung CT, LiL Chang EES, Ramsden DB, Ho SL. The interplay of aging, genetics and environmental factors in the pathogenesis of Parkinson's disease. Transl Neurodegener 2019;8:23.
[42] van Horssen J, van Schaik P, Witte M. Inflammation and mitochondrial dysfunction: a vicious circle in neurodegenerative disorders? Neurosci Lett 2019;710:132931.
[43] La Vitola P, Balducci C, Baroni M, Artioli L, Santamaria G, Castiglioni M, Cerovic M, Colombo L, Caldinelli L, Pollegioni L, et al. Peripheral inflammation exacerbates α-synuclein toxicity and neuropathology in Parkinson's models. Neuropathol Appl Neurobiol 2021;47:43–60.
[44] Yu W, Li Y, Hu J, Wu J, Huang YA. Study on the pathogenesis of vascular cognitive impairment and dementia: the chronic cerebral hypoperfusion hypothesis. J Clin Med 2022;11:4742.

[45] de Rus Jacquet A, Alpaugh M, Denis HL, Tancredi JL, Boutin M, Decaestecker J, Beauparlant C, Herrmann L, Saint-Pierre M, Parent M, et al. The contribution of inflammatory astrocytes to BBB impairments in a brain-chip model of Parkinson's disease. Nat Commun 2023;14:3651.

[46] Sheng L, Stewart T, Yang D, Thorland E, Soltys D, Aro P, Khrisat T, Xie Z, Li N, Liu Z, et al. Erythrocytic α-synuclein contained in microvesicles regulates astrocytic glutamate homeostasis: a new perspective on Parkinson's disease pathogenesis. Acta Neuropathol Commun 2020;8:102.

[47] Xiong Y, Fu Y, Li Z, Zheng Y, Cui M, Zhang C, Huang XY, Jian Y, Chen BH. Laquinimod inhibits microglial activation, astrogliosis, BBB damage, and infarction and improves neurological damage after ischemic stroke. ACS Chem Neurosci 2023;14:1992–2007.

[48] Kummer BR, Diaz I, Wu X, Aaroe AE, Chen ML, Iadecola C, Kamel H, Navi BB. Associations between cerebrovascular risk factors and Parkinson disease. Ann Neurol 2019;86:572–81.